Photosynthesis Research **22**: 257–275, 1989.

Regular paper

Photoelectric study on the kinetics of trapping and charge stabilization in oriented PS II membranes

W. Leibl[1], J. Breton[2], J. Deprez[2] & H.-W. Trissl[1]
[1]*Universität Osnabrück, Fachbereich Biologie/Chemie, Biophysik, Barbarastr. 11, D-4500 Osnabrück, FRG;* [2]*Service de Biophysique, Département de Biologie, Centre d'Etudes Nucléaires de Saclay, F-91191 Gif-Sur-Yvette Cedex, France*

Key words: annihilation, charge separation, charge recombination, exciton trapping, photosystem II, photovoltage

Abstract

Excitation energy trapping and charge separation in Photosystem II were studied by kinetic analysis of the fast photovoltage detected in membrane fragments from peas with picosecond excitation. With the primary quinone acceptor oxidized the photovoltage displayed a biphasic rise with apparent time constants of 100–300 ps and 550 ± 50 ps. The first phase was dependent on the excitation energy whereas the second phase was not. We attribute these two phases to trapping (formation of $P\text{-}680^+ Phe^-$) and charge stabilization (formation of $P\text{-}680^+ Q_A^-$), respectively. A reversibility of the trapping process was demonstrated by the effect of the fluorescence quencher DNB and of artificial quinone acceptors on the apparent rate constants and amplitudes. With the primary quinone acceptor reduced a transient photoelectric signal was observed and attributed to the formation and decay of the primary radical pair. The maximum concentration of the radical pair formed with reduced Q_A was about 30% of that measured with oxidized Q_A. The recombination time was 0.8–1.2 ns.

The competition between trapping and annihilation was estimated by comparison of the photovoltage induced by short (30 ps) and long (12 ns) flashes. These data and the energy dependence of the kinetics were analyzed by a reversible reaction scheme which takes into account singlet–singlet annihilation and progressive closure of reaction centers by bimolecular interaction between excitons and the trap. To put on firmer grounds the evaluation of the molecular rate constants and the relative electrogenicity of the primary reactions in PS II, fluorescence decay data of our preparation were also included in the analysis. Evidence is given that the rates of radical pair formation and charge stabilization are influenced by the membrane potential. The implications of the results for the quantum yield are discussed.

Abbreviations; DCBQ – 2,6-dichloro-*p*-benzoquinone, DCMU – 3-(3,4-dichlorophenyl)-1,1-dimethylurea, DNB – *m*-dinitrobenzene, PPBQ – phenyl-*p*-benzoquinone, PS I – photosystem I of green plants, PS II – photosystem II of green plants, PSU – photosynthetic unit, P-680 – primary donor of PS II, Phe – intermediary pheophytin acceptor of PS II, Q_A – primary quinone acceptor of PS II, RC – reaction center

Introduction

The early events of photosynthetic energy conversion are known to involve a series of very fast reactions. After excitation of an antenna pigment, the excitation energy is efficiently transferred to a reaction center (RC) where it is either reinjected into the antenna system or trapped by photochemistry. In this study the appearance of a charge separated state shall be defined as trapping. In PS

II charge separation involves electron transfer from the excited primary donor, P-680*, to the intermediary acceptor, pheophytin (Phe). If the one electron carrier Q_A is oxidized (open RCs), the electron is stabilized on Q_A in some hundred picoseconds (Nuijs et al. 1986, Schatz et al. 1987, Trissl et al. 1987a, Eckert et al. 1988, Trissl and Leibl 1989), thus allowing P^+ to use its oxidizing power for water cleavage. If Q_A is already reduced (closed RC) charge stabilization is no longer possible. The real fate of the excitation energy arriving at such a closed RC is still under discussion.

According to a theory first proposed by Klimov efficient radical pair formation occurs also in RCs with reduced Q_A. It is followed by a charge recombination which gives rise to a slow (2–4 ns) fluorescence decay that is not observed in open RCs (Klimov et al. 1978, Klimov and Krasnovskii 1981). In this picture the increase of the fluorescence yield upon closure of the RCs (variable fluorescence) is caused by recombination luminescence that vanishes when the state $P\text{-}680\,Phe^-Q_A^-$ is photoaccumulated at low redox potential. However, this interpretation was questioned (Moya et al. 1986, Schatz and Holzwarth 1986, Trissl et al. 1987a). Recently a detailed kinetic and energetic model for the primary reactions in PS II was formulated that gives an alternative explanation for the origin of the increased fluorescence yield upon reduction of Q_A (Schatz et al. 1988). In this model after a fast equilibration of excitation energy in the antenna system, the decay of the excited state is limited by the rate of charge separation (trap limited).

Trapping in PS II is currently considered to involve reversible processes and the RC of PS II is often called a 'shallow trap'. One argument for the reversibility is, that the excited primary donor P* is almost isoenergetic with an excited antenna molecule, Chl *a** (Van Gorkom 1985, Schatz et al. 1988). Another argument is that also the charge separated state lies energetically not far below the excited state of P-680 and the antenna ensemble and that recombination leads with a finite yield to the reformation of Chl *a** (Van Gorkom 1985, Schatz et al. 1988).

Taking the kinetic data of single photon counting fluorescence measurements on PS II particles from *Synechococcus* sp. and assuming a value for the quantum yield of charge stabilization, Holzwarth and coworkers calculated molecular rate constants for the reversible primary processes in PS II (Schatz and Holzwarth 1986, Schatz et al. 1987, Schatz et al. 1988). They concluded, that upon reduction of the quinone acceptor the rate constant of charge separation is decreased whereas the rate constant of charge recombination is almost unaffected. This shifts the equilibrium between the concentration of the excited state and the charge separated state to the former one, and for this reason the fluorescence yield observed upon Q_A reduction increases.

Notwithstanding, whether or not charge recombination really leads to a repopulation of an excited state is still controversial (Schlodder and Brettel 1988) and a wide range of numerical values for the backreaction rate has been reported (Klimov and Krasnovskii 1982, Nuijs et al. 1986, Eckert et al. 1987, Takahashi et al. 1987, Hansson et al. 1988, Schatz et al. 1988, Schlodder and Brettel 1988). It has also been suggested, that the rate constants in the reversible scheme might not only be affected by the charge on Q_A, but also by other parameters like the membrane potential (Keuper and Sauer 1989). Although there is evidence for a reversible charge separation, the extent of this reversibility and how it is controlled in the intact system is still largely unknown.

The electrogenic processes of charge separation and stabilization are well suited to be studied by photoelectric techniques. These measurements complement fluorescence and absorbance change measurements. An advantage of photovoltage measurements is that excitonic states (non-electrogenic) do not interfere with the electric signals. Recently we reported on a PS II-photovoltage in light-gradient experiments, that could be observed only in chloroplasts with destacked thylakoids but not with stacked thylakoids (Trissl et al. 1987a). The lack of a photovoltage was explained by an excitonic shortcircuit across the appressed grana membranes: The fast equilibration of excitation energy smears out the light gradient asymmetry. This shows that the energy exchange between different PS II units (lake model) extends also across neighbouring membranes.

To study PS II photochemistry by a photoelectric method one has to look for an appropriate preparation. The ideal preparation should show no PS I contamination, no excitonic shortcircuit, and

a good signal to noise ratio. These conditions were found to be best met by a pure PS II preparation (BBY-membranes), the membranes of which were destacked by a mild trypsin digestion and oriented by an electric field (Trissl and Leibl 1989).

In this study we used this preparation to investigate with high time resolution the kinetic properties of the photovoltage induced by single picosecond flashes. The much better signal to noise ratio obtained with oriented membranes as compared to the light-gradient effect allowed the application of low excitation energies and a refined kinetic analysis. Compared with the various particle preparations currently used, this preparation is probably nearer to the intact system.

Materials and methods

Oxygen-evolving PS II particles were prepared from peas (*Pisum sativum*) according to the procedure described by Berthold et al. (1981) with the modifications described by Ono and Inoue (1985). For trypsination the fragments were diluted in low salt resuspension medium to a chlorophyll concentration of 100 μg/ml and incubated in darkness at room temperature with 2 μg/ml trypsin from bovine pancreas purchased from Sigma. After 5 min the proteolytic treatment was stopped by addition of trypsin inhibitor (Sigma) in 20-fold excess and the preparation was concentrated by centrifugation. For the experiments, the chlorophyll concentration was adjusted to 2 mg/ml. With the optical path length of 0.1 mm this yields an optical density of about 0.1 at 530 nm. The preparation was checked for a possible PS I contamination by spectroscopic measurements of the absorbance change at 700 nm. The PS I content was found to be $< 5\%$.

The excitation source for the photovoltage measurements was a Q-switched or mode locked Nd-YAG laser equipped with a pulse clipping system to select single 30-ps pulses. The laser flashes (532 nm) were sent through a scatter plate in order to achieve homogenous illumination of the sample. The repetition rate was 0.1 Hz. Variation of excitation energy was done by neutral density filters. For background illumination a modified slide projector was equipped with a wide band interference filter (530–570 nm).

Reversible orientation of the PS II-membranes was carried out in the micro-coaxial cell described elsewhere (Trissl et al. 1987b) by applying small electric field pulses (120 V/cm, 30 ms) through a bias-DC-T blockpiece (model 5550; Picosecond Pulse Labs). The flash was given during the DC-orientation pulse. Alternatively the membranes were sedimented on one electrode by a short DC-pulse of up to 900 V/cm. The latter method was used if a sample with higher ionic strength (due to addition of salt or redox chemicals) had to be used. In this case chemicals were added after orientation. Except for a larger amplitude from the electrically sedimented membranes, no differences were observed between reversible and irreversible orientation.

For experiments with high time resolution the photovoltage signal was fed into 50-Ω preamplifiers (Hahn-Meitner-Institut, Berlin; frequency range 20 kHz–8 GHz) and recorded with a digital 7-GHz oscilloscope (Textronix, 7250). The instrumental signal transmission characteristics were deduced from the measurement of the ultrafast charge separation in oriented purple membranes from *Halobacterium halobium* (Zinth et al. 1985, Trissl et al. 1989). Analysis of the PS II kinetics was done by iterative convolution of a trial function with the time response of the apparatus varying a minimal number of parameters. Minimum χ^2-values and residual plots were used as criteria for optimation. Further details of data analysis have been described previously (Trissl et al. 1987a).

To compare directly the effect of long and short flashes we used a custom-built impedance converter (input resistance *ca.* 18 kΩ, limiting frequency 500 MHz) connected to a 50-Ω preamplifier (Nucletudes S.A., Orsay, France; frequency range 10 MHz–6 GHz). For these measurements on a slower time scale, the higher input impedance of the amplifier is necessary to slow down the RC-discharge time of the capacitative measuring cell. These signals were recorded with a 1-GHz oscilloscope (Tektronix, 7104) equipped with a digitizing camera (Thomson CSF, TSN 1150).

Measurements of fluorescence decay kinetics were performed with the 7-GHz apparatus described above, replacing the measuring cell by a picosecond photodiode (Coherent, Picosecond diode, rise time < 120 ps, FWHM 175 ps). Wavelengths > 665 nm were selected by an edge filter

(RG 665). The sample cuvette had a thickness of 0.1 mm and the concentration of the sample was the same as in the photovoltage measurements.

Results

Flash excitation of BBY-membranes (not trypsinated) in the microcoaxial cell did not exhibit a photovoltage even if an orienting voltage was applied. We interpret this as an ultrafast excitonic shortcircuit across the partition gap between two appressed membranes or several stacked membranes that, like in grana stacks (Trissl et al. 1987a), prevents a light-gradient photovoltage.

After a mild trypsin treatment of the membranes there was still no light-gradient photovoltage, but with electric orientation a photovoltage of several millivolts could be measured (Fig. 1a). We attribute the absence of a photovoltage to the isotropic distribution of separated membrane sheets and its presence to an orientation of the single membranes by the electric field due to an asymmetric surface charge density. This interpretation is substantiated by the finding of inverted photovoltage signals upon reversal of the orienting voltage. The polarity of the photovoltage was always opposite to the orientation polarity. This means that, at least after trypsin treatment, the acceptor side of the photosynthetic membrane must have a higher negative surface charge than the donor side.

The membranes could repeatedly be oriented with small electric pulses in the range of 40–120 V/cm for 30 ms as shown by the reversed photovoltage upon successive pulses of opposite polarity. In contrast, orienting voltages of 500–900 V/cm for several hundred milliseconds led to an irreversible sedimentation. The approximately twofold larger photovoltage amplitude observed in the case of irreversible orientation indicates that under the reversible conditions the membranes are not completely oriented. Irrespective of the kind of orientation the kinetics of the photovoltage were not affected by the electric field.

Kinetics of the photovoltage

Figure 1 shows typical time courses of the photovoltage induced by single 30-ps flashes recorded with the 7-GHz setup at a medium excitation energy. The left trace corresponds to RCs open before the flash, whereas the right trace corresponds to RCs in which Q_A was kept in the

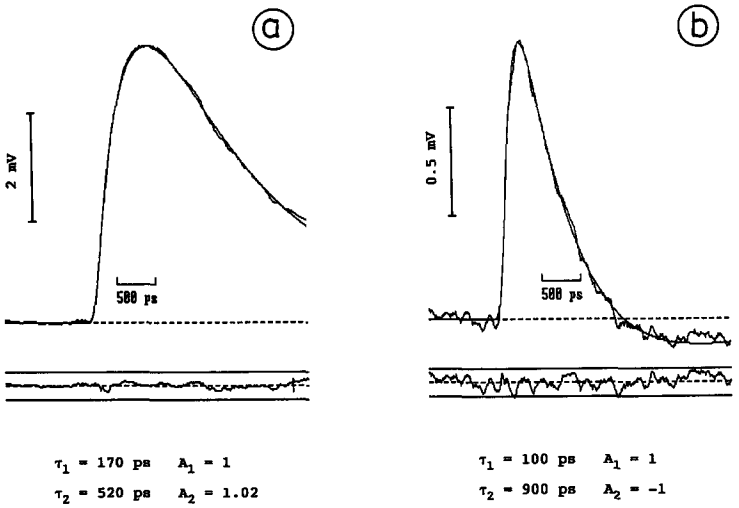

Fig. 1. Kinetics of the photovoltage in the case of open (a) and closed (b) RCs. The traces are normalized (see scaling). Excitation by 30-ps flashes of 90 μJ/cm^2. Reduction of Q_A was achieved by addition of 100 μM DCMU and continuous background illumination (0.5 mW/cm^2). Averages of 10 traces. Smooth lines are best fits of an irreversible two step reaction with time constants and relative electrogenicity factors as stated. In the fit to trace (b) 9% of the kinetic characteristics of trace (a) was added to account for uncomplete reduction. The deviation between calculated and experimental traces is shown as a residual plot below the individual traces with the straight lines indicating $\pm 5\%$ deviation.

reduced state by addition of DCMU and background illumination. No differences were observed when the RCs were closed by addition of dithionite (20 mM, pH 7.8) instead of DCMU. The measured photovoltage results from the convolution of the molecular displacement current with the apparatus response function. The latter is given by the integrating property of the capacitative measuring cell (rising phase) and its differentiating property (discharge characteristics, RC-decay) as described previously (Deprez et al. 1986, Trissl et al. 1987a). In the case of open RCs two rising phases are clearly time resolved, whereas in the case of reduced Q_A a single fast rise is followed by an accelerated decay. A kinetic analysis of numerous traces showed that within the experimental accuracy the generating function for the photovoltage (i.e. the displacement current) is well described by a sum of two exponentials:

$$I(t) = a_1 \exp(-t/\tau_1) + a_2 \exp(-t/\tau_2). \quad (1)$$

As shown in the Appendix for low excitation energy this structure of the equation is predicted from an irreversible as well as from a reversible reaction scheme. In both models the time courses of the states involved are described by the apparent time constants ($\tau_i = 1/\gamma_i$). Note that the amplitude factors have different meanings in both models.

If the amplitudes are normalized this yields three fit parameters, two exponential time constants and one relative amplitude. We want to emphasize that the interpretation of these fit parameters depends on the assumed reaction scheme (see Discussion and Appendix).

To quantify the energy dependence of the photovoltage kinetics and to keep the number of fit parameters as small as possible we used the simplest case of an irreversible reaction scheme for the approximate analysis of the photovoltage kinetics. Therefore in the following the ratio of the electrogenicity of two electrogenic steps in the irreversible reaction scheme, A_2^{irr}, is taken as a measure of the relative amplitude of the second exponential phase ($A_1 = 1$). The amplitude factors a_1 and a_2 in Eq. (1) are replaced by A_2^{irr} according to

$$a_1 = k_1/(\gamma_1 - \gamma_2)[\gamma_1 - (A_2^{irr} + 1)\gamma_2], \quad (2a)$$

$$a_2 = k_1/(\gamma_1 - \gamma_2)\gamma_2 A_2^{irr}. \quad (2b)$$

If one includes the common factor k_1 in the proportionality constant of the photovoltage amplitude, the fit parameters γ_1, γ_2 and A_2^{irr} are left. With the definition of the electrogenicity factors given in the Appendix one expects $A_2^{irr} = -1$ for a backreaction. The smooth lines in Fig. 1 represent the best fit as obtained by convolution of the generating function [Eq. (1)] with the response function of the apparatus (Materials and Methods). The deviation between calculated and experimental traces is shown as a residual plot below the individual traces with the straight lines indicating $\pm 5\%$ deviations.

At the excitation energy of 90 μJ/cm^2, the fit yielded for open RCs $\tau_1 = 170$ ps, $\tau_2 = 520$ ps and $A_2^{irr} = 1.02$ and for reduced RCs $\tau_1 = 100$ ps and $\tau_2 = 900$ ps. In the case of reduced Q_A the maximum amplitude of the photovoltage signal was diminished to 10%–20% of the maximum amplitude of oxidized samples and the relative amplitude A_2 of the three-parameter fit yielded $A_2^{irr} = -0.80$ to $A_2^{irr} = -0.90$. Good fits with the expected value of $A_2 = -1$ for a simple backreaction became possible by admixing a small amount (10%) of oxidized centers.

In analogy to the findings in purple bacteria (Deprez et al. 1986, Dobek et al. 1989) we interpret the fast rise in open and closed RCs as the appearance of the electrogenic charge separated state between the primary donor P-680 and the intermediary acceptor pheophytin (Trissl et al. 1987a, Trissl and Leibl 1989), and the slow rise as the electrogenic step of charge stabilization on the primary quinone acceptor Q_A. In the case of reduced Q_A the latter reaction is absent and the accelerated decay is interpreted as a backreaction (charge recombination). In the following we will call the apparent time constant of the fast phase 'trapping time'.

Dependence of the kinetics on the excitation energy

The analysis [according to Eq. (1)] of the photovoltage at different excitation energies showed that in open RCs only the fast phase is considerably influenced whereas the time constant and the relative amplitude of the slow phase remain virtually constant ($\tau_2 = 500$–600 ps, $A_2^{irr} = 0.9$–1.2). Figure 2

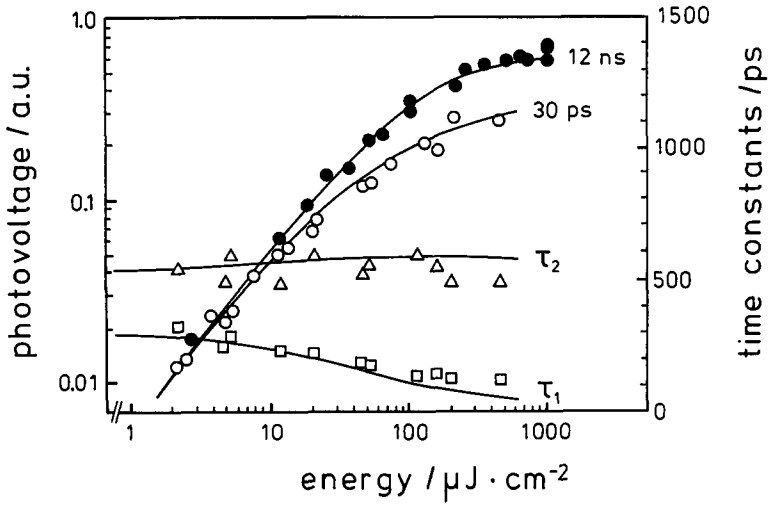

Fig. 2. Energy dependence of the photovoltage amplitude for excitation of dark-adapted membranes with 12-ns flashes (filled circles) and 30-ps flashes (open circles). Energy dependence of the apparent time constants resulting from a fit by two exponentials (fast phase: squares, slow phase: triangles). The solid lines give the best simultaneous fit to these data and the data in Fig. 3 with the parameters in Table 3 according to Eqns. (5)–(7).

(squares) shows the dependence of the fast rise time on the excitation energy. In the low energy limit the time constant approached a value of 300 ± 30 ps. An increase of the excitation energy caused a strong decrease of this time constant.

In the case of closed RCs at comparable excitation energies the first phase was found to be faster than in open RCs (squares in Fig. 3). The decay time decreased slightly with increasing excitation energy (triangles in Fig. 3).

Competition between trapping and annihilation

The previous experiments with picosecond excitation clearly show, that the kinetics of the primary

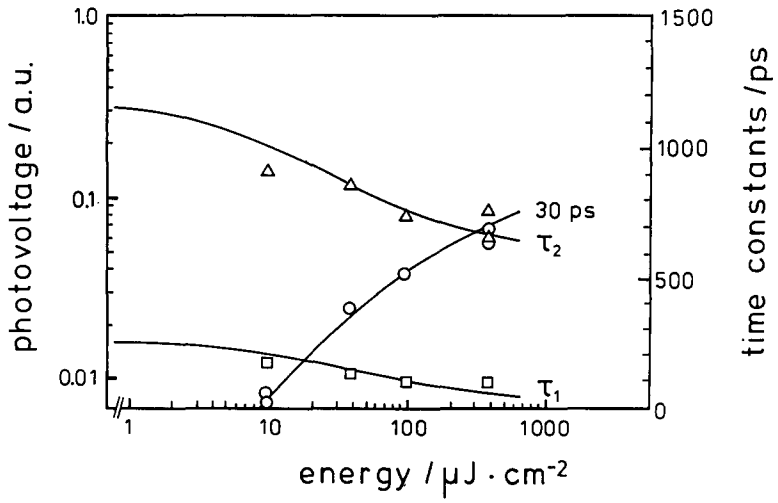

Fig. 3. Energy dependence of the photovoltage amplitude (open circles) and kinetics upon closing the RCs by DCMU and background light (rise time: squares, decay time: triangles). Excitation by 30-ps flashes. The solid lines give the best simultaneous fit to these data and the data in Fig. 2 with the parameters in Table 3 according to Eqns. (8)–(10).

reactions are governed by the exciton density. In addition to the monomolecular loss processes in the antenna that are independent of the excitation energy, in the case of high intensity picosecond flashes also losses by bimolecular exciton–exciton annihilation occur. Annihilation effects become relevant if the excitation density is high enough to create on the order of one exciton or more per domain (Geacintov and Breton 1987) in a time interval comparable to the lifetime of the excitons. In order to quantify the extent of losses due to singlet–singlet annihilation at high excitation density, we compared the amplitude of the photovoltage evoked by short and long laser flashes. These experiments were made with the 1-GHz setup as described in Materials and Methods. Figure 2 shows in a double logarithmic plot the energy dependence of the maximum photovoltage amplitude induced by 12-ns flashes (closed circles) and 30-ps flashes (open circles). It can be seen, that for an excitation energy of more than about $10\,\mu J/cm^2$ there is a marked loss of photovoltage amplitude with picosecond excitation reaching a factor of 2 at energies higher than $150\,\mu J/cm^2$.

Influence of the fluorescence quencher DNB, artificial acceptors and ionic strength

To distinguish between a reversible and irreversible reaction mechanism of the primary reactions we chose a threefold approach. First, with the addition of an artificial fluorescence quencher we introduced a change on the left side of the reaction scheme (see Discussion), namely an additional decay path for the excitons in the antenna that, by competing with trapping, should lead to a decreased photosynthetic quantum yield. Second, with the use of artificial acceptors we introduced a change on the right side of the reaction scheme. Third, we increased the salt concentration to diminish the surface potential of the membrane fragments.

Figure 4 shows typical examples of the kinetics in open RCs after addition of 4 mM DNB (a), or 1 mM DCBQ (b), or 20 mM $CaCl_2$ (c). For comparison, the fit curves describing the photovoltage from samples without any addition (Fig. 1a) are overlayed. In all three cases the kinetics and/or the amplitude of the photovoltage are significantly changed. DNB decreased the amplitude by a factor of 3, whereas DCBQ increased it by a factor of 1.3 to 1.6 depending on the preparation and excitation energy. All added chemicals accelerated the fast rise time and decreased the time constant of the slower phase. With other artificial acceptors like PPBQ and $K_3[Fe(CN)_6]$ or with lower salt concentrations the effect was in the same direction although not as distinct. In the presence of DNB also the apparent decay of the radical pair in the reduced RCs was accelerated (data not shown). The parameters ob-

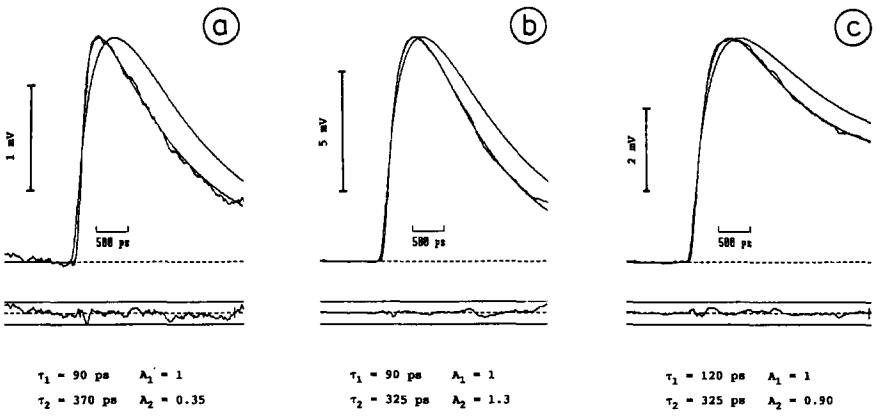

Fig. 4. Kinetics of the photovoltage after addition of the artificial fluorescence quencher DNB (a), the artificial acceptor DCBQ (b), and $CaCl_2$ (c). The traces were normalized to equal height. Concentrations used: 4 mM DNB, 1 mM DCBQ, *ca.* 20 mM $CaCl_2$. Excitation by 30-ps flashes of $90\,\mu J/cm^2$. Averages of 10 traces. Smooth lines are best fits of an irreversible two step reaction with time constants and relative electrogenicity factors of the second step as stated. The calculated kinetics of the photovoltage with the fit parameters obtained without any addition (Fig. 1a) is overlayed. The slower decay time of the signal at high ionic strength is due to electrode/electrolyte interaction.

tained from the kinetic fit procedure are summarized in Table 1. All values in Table 1 are deduced from experiments at the same excitation energy of 90 $\mu J/cm^2$.

Fluorescence

To obtain additional and independent information on energy migration and trapping by RCs in the preparation used we also measured the fluorescence decay kinetics with picosecond excitation close to the low energy limit. The time resolution was given by the response function of the photodiode (175 ps FWHM). The data were analyzed by convolution of a sum of two or three exponentials with the apparative response function. An analysis with a third phase always displayed amplitudes for this phase of $< 5\%$ with insignificant changes of the parameters of the two component analysis. Therefore a two exponential analysis was sufficient. Exponential phases as short as 40 ps could be resolved.

Figure 5 shows kinetic traces of the fluorescence decay of the sample with open RCs (a), closed RCs (b), with DNB (c), and with DCBQ (d). The results of the kinetic analysis are summarized in Table 2 which also includes the fluorescence yield calculated by $\Phi^{fl} = k_{rad}(a_1^{fl}\tau_1 + a_2^{fl}\tau_2)$, where k_{rad} is the natural fluorescence lifetime $[k_{rad} = (15\,ns)^{-1}]$.

Table 1. Apparent time constants and relative amplitudes as derived from the photovoltage kinetics under different experimental conditions at the excitation energy of 90 $\mu J/cm^2$ applying the irreversible reaction scheme to evaluate A_2^{irr}. The experimental error in the analysis was $\pm 5\%$.

Addition	τ_1 ps	τ_2 ps	A_2^{irr}	A_{max} [a]
None	170	520	1.02	1
DCMU + light	100	900	−0.9	0.1–0.2
Dithionite	110	1100	−0.85	0.1–0.2
$K_3[Fe(CN)_6]$	100	340	1.4	1.4
PPBQ (1 mM)	95	350	1.5	1.3
DCBQ (1 mM)	90	325	1.3	1.5
DNB (4 mM)	90	370	0.35	0.35
DNB + light	85	400	−0.9	–
$CaCl_2$ (20 mM)	110	325	0.9	–
NaCl (10 mM)	120	420	1.1	–

[a] The maximum photovoltage amplitude is given relative to the photovoltage without addition and is corrected for the apparative transmission characteristics.

The most interesting features are: (i) With open RCs (no addition of chemicals) the decay is described by two phases with time constants of $\tau_1 = 220$ ps and $\tau_2 = 630$ ps with relative amplitudes of 64% and 36%, respectively (Fig. 5a). (ii) With closed RCs a slow phase with a time constant of approximately 1.25 ns (58%) becomes dominant over a fast phase of 275 ps (42%) (Fig. 5b). (iii) If DNB or DCBQ is present, the slow phase in open RCs is nearly completely suppressed ($< 5\%$) and the fast phase accelerated to 75–95 ps (Fig. 5c, d). In the presence of DNB the addition of 10 mM dithionite has almost no effect (data not shown). (iv) There is not much difference between the fluorescence characteristics of trypsinated and un-

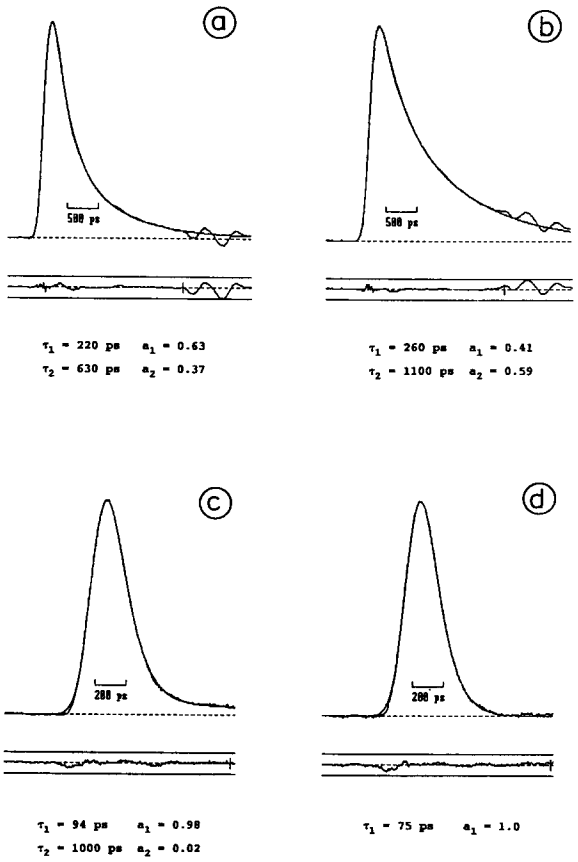

Fig. 5. Kinetics of the fluorescence decay after excitation with a 30-ps flash of 8 $\mu J/cm^2$. (a) no addition, (b) 100 μM DCMU and background illumination, (c) 4 mM DNB, (d) 1 mM DCBQ. Averages of five traces. Smooth lines represent the best fit of two exponential phases with the time constants and relative amplitudes as stated. Note the different time scale in (c, d).

Table 2. Decay times, relative amplitudes, and yields of the chlorophyll fluorescence under different experimental conditions analyzed by the sum of two exponentials. The experimental errors for different samples were for the time constants ± 10% (of the value) and for the amplitudes ± 3% (absolute)

Addition	τ_1 ps	a_1^{fl} %	τ_2 ps	a_2^{fl} %	Φ_{fl} %
Trypsinated BBY-membranes:					
None	220	64	630	36	2.4
DCMU + light	260	41	1200	59	5.0
Dithionite	290	42	1300	58	5.8
$K_3[Fe(CN)_6]$	180	83	600	17	1.7
PPBQ (1 mM)	105	99	(1500)[a]	< 2	0.8
DCBQ (1 mM)	75	100			0.5
DNB (4 mM)	95	95	(1000)	< 5	0.7
DNB + dithionite	92	99	(480)	< 5	0.7
Not trypsinated BBY-membranes					
None	240	57	600	43	2.6
+ light	270	37	1200	63	5.7

[a] Numbers in brackets are estimations because of the small amplitudes.

trypsinated membranes (see Table 2), indicating that energy migration and trapping in our PS II membrane preparation are not much affected by the mild trypsination.

The ratio of the fluorescence yields in oxidized and reduced samples calculated from the kinetics was also found by fluorescence induction measurements (data not shown).

Discussion

The separation of PS II membranes by trypsination

The appearance of a photovoltage after trypsination demonstrates the cancellation of the excitonic shortcircuit between two antiparallel appressed membrane sheets, that could not be achieved by simply washing the membranes in low salt buffer. It is well known that there is a polypeptide on the light harvesting complex (LHC) of PS II that is essential for stacking (Carter and Staehelin 1980, Mullet and Arntzen 1980), that this polypeptide is positively charged, and that it can be removed by mild trypsin digestion (Steinback et al. 1979, Mullet 1983). In the intact system this residue controls the distribution of excitation energy between PS I and PS II by its phosphorylation which in turn is controlled by the redox state of the plastoquinone pool (Allen et al. 1981).

Because mild trypsination is highly specific for this polypeptide (Steinback et al. 1979), we attribute the finding of trypsin induced membrane separation to the removal of this polypeptide that is known to be responsible for the cross-membrane adhesion and to be accessible from the external surface of the thylakoid membrane. Our finding of a higher negative surface charge of the acceptor side of the membranes might be — at least in part — due to the removal of the positively charged residue from this side. The resulting electric field has the same direction as the photosynthetic charge separation and hence might diminish the quantum yield of the primary processes in the RC (see below).

Reversibility of the primary reactions

The kinetic features of the photovoltage in PS II (Fig. 1) resemble those found in purple bacteria (Deprez et al. 1986, Dobek et al. 1989, Trissl and Leibl 1989, Trissl et al. 1989): a biphasic rise in open RCs and a backreaction in closed RCs. For the charge separation in purple bacteria it was shown that an irreversible reaction scheme is adequate (Trissl et al. 1989). In the following we want to discuss our experimental results with respect to a reversibility of trapping in PS II. The experimental findings are (i) the change of kinetics and amplitude of the photovoltage by the fluorescence quencher DNB (Fig. 4a), (ii) the change of kinetics and yield of the photovoltage by artificial acceptors (Fig. 4b), and (iii) the presence of a fluorescence phase in open RCs with the apparent time constant of charge stabilization τ_2 (Fig. 5a). Here we need only a qualitative discussion of these findings and not the exact molecular parameters which we attempt to determine in the next section.

To distinguish between an irreversible and a reversible reaction scheme one has to compare the effect of the assumed reaction scheme on observable quantities. In the low energy limit the irreversible reaction can be visualized by the scheme

$$D \xleftarrow{k_3} A \xrightarrow{k_1} B \xrightarrow{k_2} C$$

and the reversible reaction by

$$D \xleftarrow{k_3} A \underset{k_{-1}}{\overset{k_1}{\rightleftharpoons}} B \xrightarrow{k_2} C$$

where A represents the state (Chl_N P-680)* (fast equilibration of excitation energy), B the charge separated state P-680$^+$ Phe$^-$, C the state P-680$^+$ Phe Q_A^- in open and P-680 Phe Q_A^- in closed RCs, respectively, and D the ground state(Chl_N P-680). The rate constant k_1 describes trapping (including energy transfer and charge separation) and k_{-1} is the molecular rate constant of detrapping, k_2 describes irreversible depopulation of the state B due to charge stabilization (open RCs) or due to other deactivation paths including charge recombination without repopulation of the excited state in the irreversible scheme (closed RCs), and k_3 all loss processes in the antenna like fluorescence and non-photochemical quenching. The solutions of the corresponding first order rate equations are given in the Appendix. Note that the second scheme can be transformed into the first one by $k_{-1} \rightarrow 0$. It should also be noted that with photovoltage measurements the time course of $B(t)$ and $C(t)$ is detected, whereas with fluorescence only $A(t)$ is measured. In the irreversible scheme $A(t)$ and $D(t)$ are monoexponential with an apparent rate constant $\gamma_1 = (k_1 + k_3)$, and $B(t)$ and $C(t)$ are biexponential with a second phase having the apparent rate constant $\gamma_2 = k_2$, whereas in the reversible scheme all concentrations show a time dependence described by two exponential phases with the same apparent rate constants given by

$$\gamma_{1,2} = \frac{\Sigma\, k_i \pm \sqrt{(\Sigma\, k_i)^2 - 4(k_{-1}k_3 + k_3k_2 + k_1k_2)}}{2}. \tag{3}$$

In the following we will check the predictions of the two models for compatibility with experimentally determined quantities. We are aware of the fact, that the use of the solutions for the low energy limit is an approximation when applied to our data collected under higher excitation energy. Therefore we took only data obtained under conditions where not more than about 20% of the RCs are closed by a flash. A comparison of the numerical solution of the general differential equation system for arbitrary energies [Eqs. (5)–(7)] with two exponentials (low energy approximation) showed that the differences are beyond the error of our analysis. Because in the approximation of the kinetics by exponential functions at least the rate constants k_1 and k_3 are expected to vary with the excitation energy (due to the bimolecular processes of trapping and annihilation), we only compare kinetics obtained under identical excitation conditions.

The addition of the fluorescence quencher DNB led to a faster fluorescence decay (Fig. 5c) and a smaller photovoltage amplitude (Fig. 4a) demonstrating an accelerated deactivation of the excitation in the antenna and a lowered photosynthetic quantum yield. This quencher is expected to increase only the value of the molecular rate constant k_3. In the irreversible scheme this has an effect only on the rate constant γ_1 of the fast phase but neither on the kinetics (γ_2) nor on the amplitude of the second phase. Hence, the observed changes of the rate constant and amplitude of the second phase (Fig. 4a and Table 1) are only comparable with the reversible scheme, in which k_3 also mixes into γ_2.

Artificial acceptors like the halogenated quinone used in this work are known to act not only on the acceptor site of PS II but are also able to quench the excited state in the antenna (Kitajima and Butler 1975, McCauley and Melis 1987, Karukstis and Monell 1989). Although with DCBQ the kinetics of both fluorescence and photovoltage look very similar to those obtained with DNB, the effect on the photovoltage amplitude is opposite: DNB decreases but DCBQ increases the photovoltage amplitude. This shows that quenching in the antenna cannot be the main effect of the artificial acceptor.

The total photovoltage amplitude is proportional to the final concentration of the charge stabilized state $C(t \rightarrow \infty)$ that in turn is proportional to the photosynthetic quantum yield, Φ_p. As shown in the Appendix the yield for the two models is given by

$$\Phi_p^{irr} = \frac{k_1}{k_1 + k_3} \qquad \Phi_p^{rev} = \frac{k_1 k_2}{\gamma_1 \gamma_2} \tag{4}$$

In the irreversible scheme it is impossible to explain an increase of the quantum yield, assuming k_1 is not influenced by the artificial acceptor, because k_3 cannot decrease. Even if k_1 and k_2 are allowed to increase in the presence of the artificial acceptor in order to model both, the increase of the quantum yield and the change in the kinetics of the second phase, then the contradiction to the observation arises, that in any case the relative amplitude of the

second phase, A_2^{irr}, must stay constant, given invariant dielectric distances.

In the reversible scheme, however, it is possible to increase the quantum yield with a reasonable choice of parameters and simultaneously be in accordance with the measured changes in the kinetics and relative amplitudes. Since $\gamma_1\gamma_2$ is a quantity that is observed to increase upon addition of the artificial acceptor (Table 1), in the above equation the product k_1k_2 must be increased even more. The model predicts that a considerable increase of the rate constant of charge stabilization, k_2, leads to a strongly increased amplitude of the slow fluorescence phase. Because this is not observed (Fig. 5d, Table 2) one can conclude that not only this but also a significant increase in k_1 must occur. Equation (A.15) in the Appendix shows, that a change in k_2 may yield also another value of the relative amplitude of the second photovoltage phase, A_2^{irr}, in accordance with the experimental observation. A more detailed treatment will be given in the next section.

A last argument in favour of the reversibility of trapping in PS II is the presence of a fluorescence phase (> 30% in our preparation) with a rate constant similar to that of the slow phase of the photovoltage. This phase is also found in single photon counting fluorescence decay measurements where it is called 'middle' phase (for a review see Van Grondelle 1985, Geacintov and Breton 1987, Van Grondelle and Sundström 1988). But it was only recently interpreted in this way (Schatz et al. 1988). Alternatively it was attributed to the trapping time in PS II_β -centres (Butler et al. 1983, Holzwarth et al. 1985) or the transfer time from different light harvesting proteins to the RC (Haehnel et al. 1982, Karukstis and Sauer 1985). With the assumption of a fast equilibration of the excitation energy in the antenna system and a homogenous population of PSUs, the biphasic fluorescence decay found in this study is only compatible with the reversible reaction scheme.

If our preparation would be heterogenous this could be reconciled with the irreversible scheme by assigning the two phases to the trapping times of two populations. Then the slow photovoltage phase should result from consecutive rather than parallel processes. This possibility can be rejected by the properties of the slow phase: It vanishes upon reduction of Q_A and it is almost independent of the excitation energy (Fig. 2). Because of the longer lifetime of the excitons in the second population, however, trapping in this population should be even more affected by annihilation, in contradiction to what is observed.

The same conclusion was drawn in a recent study of annihilation effects on the fluorescence decay kinetics by France et al. (1988). The decrease of the amplitude but not of the time constant of the slower phase with increasing excitation energy was taken as evidence for a homogenous origin of both fluorescence phases being correlated with each other.

Relations between molecular rate constants

The above arguments establish a kinetic model of the primary reactions in PS II that takes into account reversible trapping (Van Gorkom 1985, Schatz et al. 1988). In the reversible scheme the physically more meaningful molecular rate constants are hidden in two observable rate constants. Furthermore, for the evaluation of the relative electrogenicity of charge stabilization, the knowledge of the molecular rate constant k_2 is needed. To obtain basic information on the variability of the primary photochemical processes in the RC one needs only ratios of rate constants.

As shown in the Appendix [Eq. (A.13)], the formula for the maximum radical pair concentration contains k_1 as the only unknown molecular parameter, whereas the apparent rate constants are measured. If k_1 is affected by different experimental conditions this can easily be determined by means of the maximum radical pair concentration, RP_{max}. In the case of open RCs this quantity becomes accessible by a computing procedure, in which in a first step the parameters of the photovoltage kinetics are determined by a fit according to the reaction scheme, and in a second step the peak photovoltage amplitude for a vanishing electrogenicity of the second phase ($A_2 = -A_1 = -1$) [Eq. (A.14)] is determined holding all other parameters constant.

Forming the ratio of the photovoltage amplitudes belonging to the maximum radical pair concentration of oxidized (applying this procedure) and reduced samples (directly measured), we find that upon reduction of Q_A, RP_{max} is diminished by a factor of 3 and $k_1^{ox}/k_1^{red} = 3.2 \pm 0.7$. This shows

that the field induced by the charge on Q_A controls the trapping rate as suggested by Schatz et al. (1987). For the DNB experiments we obtained $k_1(+\text{DNB})/k_1(-\text{DNB}) = 1.0$. Since DNB is expected not to influence the trapping rate constant, this finding gives confidence in the analysis. The analogous calculation for the DCBQ experiments yields $k_1(+\text{DCBQ})/k_1(-\text{DCBQ}) = 2.1$. A similar ratio is found for ferricyanide experiments, $k_1(+\text{K}_3[\text{Fe(CN)}_6])/k_1[\text{Fe(CN)}_6]) = 1.9$. These surprising increases of the trapping rate could be ascribed to a conformational change in the RC polypeptides as reported (Trebst et al. 1988) or, more likely, to a change of the redox state of the non-haem iron from Fe^{2+} to Fe^{3+} (Zimmermann and Rutherford, 1986).

As can be shown [Appendix Eqs. (A.11) and (A.13)], a change of the rate constant k_2 can be detected by comparing the ratio RP_{max}/Φ_p^{rev} under different experimental conditions. Taking the four meaured rate constants and determining RP_{max}/Φ_p^{rev} as mentioned before this yields $k_2(+\text{DCBQ})/k_2(-\text{DCBQ}) = 2.0 \pm 0.3$ and $k_2(+\text{K}_3[\text{Fe(CN)}_6])/k_2(-\text{K}_3[\text{Fe(CN)}_6]) = 1.9$. This ratio can be calculated independently from the fit parameters γ_2 and A_2^{irr} [Eq. (A.15) in the Appendix] which yields the same numerical values. The latter calculation is the only way to determine a change of k_2 when the ionic strength is varied because the addition of salt influences the photovoltage amplitudes due to a disturbed orientation of the membranes. The decreased value of $(A_2^{irr} + 1)\gamma_2$ found at higher ionic strength implies an increase of the rate constant of charge stabilization k_2 by a factor of $k_2(+\text{salt})/k_2(-\text{salt}) = 1.9 \pm 0.3$.

The effect of artificial acceptors on k_2 can be explained similarly as its effect on k_1, namely by a conformational change or a modified redox state of the quinone-iron site. The faster charge separation causes a faster depopulation of the excited state, as becomes obvious by the lowered fluorescence yield (Table 2). The increase of k_2 by an increase of the ionic strength we ascribe to a decreased transmembrane potential, which is built up by the asymmetric negative surface charge density of the open membrane sheets. Ca^{2+} is known to reduce the surface charge density and the concomitant higher ionic strength decreases the surface potential. Both effects diminish the transmembrane potential. The change of k_2 is in the expected direction, since the electron transfer is directed against the transmembrane potential, as known from the relation of the polarities of the photovoltage and the orienting voltage (see Results). Similar conclusions have been drawn earlier (Meiburg et al. 1983, Drechsler and Neumann 1987). In chloroplasts a corresponding effect of low ionic strength (destacking conditions) on the kinetics of the primary reactions in PS II may be masked by energy transfer to PS I, which is a much stronger quencher.

Determination of molecular rate constants

For a unique extraction of molecular rate constants in the case of reversible reactions many experimental observables are necessary. With the different dependencies available in the present work (excitation energy, flash duration, DNB, artificial acceptors, ionic strength), this is possible.

To describe the primary photochemistry of PS II at arbitrary excitation conditions one needs a kinetic model that takes into account the reversibility of trapping, exciton–exciton annihilation, and the change of the fraction of open RCs during the lifetime of the excitons. With such a model and by a global fit to all our data the molecular rate constants involved will be determined.

For the following set of differential equations we use the same nomenclature as for the reversible reaction scheme in the low energy limit. The effect of annihilation is accounted for by the overall bimolecular decay rate constant γ as defined by Paillotin et al. (1979). Under the assumpions of a lake model organization of PSUs that is well established for PS II (Geacintov and Breton 1987), and of a complete equilibration of the excitation energy (i.e. reaction limited trapping) the differential equations read in the case of open RCs:

$$dA/dt = -k_1(1 - B - C)A + k_{-1}B - k_3A - \gamma/2A^2 - k_c(B + C)A \quad (5)$$

$$dB/dt = k_1(1 - B - C)A - k_{-1}B - k_2B \quad (6)$$

$$dC/dt = k_2B \quad (7)$$

and in the case of closed RCs

$$dA/dt = -k_1(1 - B)A + k_{-1}B - k_3A - \gamma/2A^2 - k_cBA \quad (8)$$

$$dB/dt = k_1(1 - B)A - k_{-1}B - k_2B \quad (9)$$

$$dC/dt = k_2B \quad (10)$$

in which k_c is the quenching rate constant of the states P-680$^+$ Phe$^{(-)}$ $Q_A^{(-)}$. In general the values of the rate constants k_i may be different in open and closed RCs. The equations were solved numerically with the initial conditions $A(0) = z$, $B(0) = C(0) = 0$, expressing the excitation energy by the number of hits per PSU, $z = N\sigma E$, where E is the excitation energy, N the number of Chl/RC (= antenna size), and σ the mean absorption cross section of a single antenna chlorophyll at 532 nm. The case of 30-ps excitation was approximated by the initial condition $A(0) = z$ (corresponding to δ-function excitation) and the case of 12-ns excitation by a distribution of the energy into 10 δ-function pulses and an iterative calculation of the photovoltage. This procedure accounts for some spike structure of our Q-switched laser pulse.

The solutions of the differential equations are not analytical functions and therefore no exact apparent rate constants can be calculated. To match the predicted numerically calculated time courses to the photovoltage kinetics, the same two-exponential fit procedure was applied to the numerical solutions as was applied before to the photovoltage signals. The approximation of the numerical solutions by two exponential terms is very good at low energies and does not exceed $\pm$ 5% deviations at the highest energy tested. In the low energy limit the differential equations yield apparent rate constants which correspond to those given by Eq. (3).

For a simultaneous fit of the kinetics and amplitudes of our photovoltage and fluorescence experiments, the following restrictive, but reasonable assumptions were made: the invariance of the annihilation parameter γ, of the electrogenicity of the second electron transfer step A_2^{rev}, of the antenna size N, and of the maximum photovoltage obtained if all RCs were transferred into the state P-680$^+$ Q_A^- by a flash. The rate constant for losses in the antenna, k_3, is assumed to be about the same for oxidized and reduced RCs. DNB only affects k_3.

It turned out that some parameters can be determined more precisely than others. For example, (i) the trapping and detrapping rate constants k_1 and k_{-1} in open and closed RCs are confined by γ_1 at low excitation energy and the relative amplitude of the second fluorescence phase; (ii) the detrapping rate constant k_{-1} is confined by the difference between γ_1 and γ_2 and the variation of γ_2 with the excitation energy. (iii) the rate constant of charge stabilization k_2 is confined by the change of γ_2 due to DNB. (iv) The relative electrogenicity A_2^{rev} is confined by the product $(A_2^{irr} + 1)\gamma_2$ and the value of k_2 [see Eq. (A.15) in the Appendix]. (v) The annihilation parameter γ and the antenna size N are confined by the data in Figs. 2 and 3. Further restrictive conditions for the determination of the parameters are the kinetic phases of fluorescence and the ratio $F_{max}/F_0 = 2.5$ found by fluorescence induction measurements.

With $\sigma = 1.6 \times 10^{-17}$ cm^2 (Geacintov and Breton 1982, our own measurements) good fits to all results were obtained for a maximum amplitude of $V_0 = 7$ mV and an antenna size of $N = 200 \pm 20$. With these numbers one hit per RC ($z = 1$) corresponds to 120 μJ/cm^2. The analysis showed that k_c had little influence on the quality of the fits. Hence, the quenching power of the states P-680$^+$ Phe$^{(-)}$$Q_A^{(-)}$, k_c, remains undetermined within the range $k_c = (300\text{–}750\,\text{ps})^{-1}$. The other parameters are summarized in Table 3 and are used for the fits in Figs. 2 and 3 (solid lines).

In a previous study Schatz et al. (1988) quoted corresponding molecular rate constants for oxygen-evolving PS II particles from *Synechococcus* sp. with about 80 Chl/P-680. They found a 6-fold decrease of the rate constant of radical pair formation after reduction of Q_A ($k_1^{ox}/k_1^{red} = 6$), whereas the rate constant of detrapping was only slightly increased ($k_{-1}^{ox}/k_{-1}^{red} = 0.9$) as reflected by the 2.5-fold increase of the apparent trapping time ($\gamma_1^{ox}/\gamma_1^{red} = 2.5$). Our data also show a strong decrease of the rate constant of trapping ($k_1^{ox}/k_1^{red} = 3$), which can be considered to be compatible to the data of Schatz et al. if the effect of ferricyanide (used in their work) on k_1 is taken into account. However, at variance is the drastic increase of the rate constant of detrapping reported here ($k_{-1}^{ox}/k_{-1}^{red} \approx 0.15$). In line with this is the slightly decreased apparent trapping time when the RCs are closed ($\gamma_1^{ox}/\gamma_1^{red} \approx 0.8$).

Table 3. Molecular parameters according to a reversible reaction scheme [Eqs. (5)–(10)] for PS II membranes at low salt concentration with oxidized (ox.) and reduced (red.) Q_A, and at high salt concentration with oxidized Q_A (+ salt), as well as the value of the rate constant k_3 after addition of 4 mM DNB (+ DNB). For some parameters the error is larger if within a certain limit a change of this parameter can be compensated by a change of another parameter.

	$1/k_1$ ps	$1/k_{-1}$ ps	$1/k_2$ ps	$1/k_3$ ps	A_2^{rev}	$1/\gamma$ ps
ox.	520 ± 40	2500 ± 500	510 ± 40	1000^{+500}_{-100}	0.85 ± 0.05	74 ± 6
red.	1560 ± 200	330 ± 40	2800 ± 800	1100^{+300}_{-100}	-	74 ± 6
+ salt	300 ± 30	2600 ± 600	280 ± 40	1100^{+500}_{-100}	0.85 ± 0.05	
+ DNB				150 ± 20		

A comparison of the numerical values of rate constants quoted by Schatz et al. (1988) and those found by us shows, that for open RCs the reversibility (k_{-1}) in our preparation is less pronounced. The opposite is found for closed RCs. The strongly reduced maximum radical pair concentration in the case of reduced Q_A is fully consistent with the idea, that the equilibrium of the excitation energy is shifted to the antenna side (Van Gorkom 1985, Schatz et al. 1988) and that it is regulated by the redox state of the RC. All these experimental findings can only be reconciled with a trapping mechanism that is limited by the photochemistry in the RC.

If the RC of PS II constitutes a shallow trap in an almost homogeneous antenna and trapping is limited by the intrinsic (i.e. molecular) rate constant of charge separation, k_1^{int} (Schatz et al. 1988), the latter can be estimated. Under these conditions the probability of the excitation energy to reside on the primary donor is on the order of $1/N$ and, if the small energetic difference between Chl a* and P-680* is neglected (the maximum absorption of our preparation lies at 679 nm), the approximation $k_1^{int} \approx Nk_1$ holds (Pearlstein 1982). With the assumption of a homogeneous antenna of $N = 200$ we calculate the molecular rate of charge separation to $k_1^{int} \approx (2.75\,ps)^{-1}$. This is in reasonable agreement with picosecond absorption measurements in isolated PS II RCs (Wasielewski et al. 1989) and a similar estimation made by Schatz et al. (1988). For the reduced case we calculate $k_1^{int} \approx (7.8\,ps)^{-1}$.

The numbers quoted in Table 3 allow to calculate the maximal radical pair yield in the reduced case to be 10%. Considering the relative electrogenicity and the convolution with the apparatus response this yields an amplitude of the photovoltage of about 10–15% of that with open RCs. This small signal was below the detection limit of the light-gradient experiments on a barley PS I-mutant (Trissl et al. 1987a). With the correlation between the rate constant of trapping and the antenna size given before it is possible to predict from our data a 2.2-fold increase of the maximum radical pair concentration in the reduced case when the antenna size decreases from 200 to 80 [Eq. (A.13)]. This compares well with the radical pair yield of 23% measured spectroscopically by Schatz et al. (1988).

As seen in Table 3, k_1 and k_2 increase at higher ionic strength. We interpret this finding as the effect of the transmembrane potential on the kinetics of the two electrogenic steps of charge separation and thereby also on the photosynthetic quantum yield in PS II. If this is true, one would expect a longer trapping time when already a larger fraction of RCs is closed, due to the counteracting field induced by the closure of neighbouring RCs. This occurs during the lifetime of excitons in high energy flashes and may be the reason for the deviations of the trapping times found at high excitation energy in Fig. 2. Our interpretation is in line with the conclusions of Keuper and Sauer (1989). It is also supported by fluorescence decay measurements of *Scenedesmus obliquus* in which the middle phase increases and the fast phase decreases upon the transition from state I to state II, the latter being connected with a phosphorylation of the light-harvesting protein on the acceptor side (Wendler and Holzwarth, 1987).

Given the assumption made before of complete equilibration of the excitation energy, the values for the rate constants of trapping, k_1, and detrapping, k_{-1}, (Table 3) allow to calculate the free energy changes of the different states. In our preparation with an antenna size of $N = 200$ we find for the reactions

$$(Chl_N\,P\text{-}680)^*\,Phe\,Q_A \rightleftharpoons Chl_N\,P\text{-}680^+\,Phe^-\,Q_A$$

$$(Chl_N\,P\text{-}680)^*\,Phe\,Q_A^- \rightleftharpoons Chl_N\,P\text{-}680^+\,Phe^-\,Q_A^-$$

$\Delta G_{ox} = -39 \pm 6$ meV and $\Delta G_{red} = +38 \pm 7$ meV, respectively. Hence the effect of Q_A-reduction lifts the radical pair state by $\approx +77$ meV. This shift is more than the 50 meV reported by Schatz et al. (1988).

Competition between trapping and annihilation

The competition between trapping and annihilation is best seen by the difference between the photovoltage amplitude evoked by 12-ns and 30-ps flashes (Fig. 2). For the energies and duration of the excitation pulses used in this study only singlet–singlet annihilation is expected (Geacintov and Breton 1987). The global analysis (Table 3) yielded an annihilation parameter $\gamma = (74\,\text{ps})^{-1}$. Often a bimolecular rate constant is quantified which is defined as $\gamma' = \gamma v = \gamma N/c_M$, where v is the volume of a PSU and c_M the concentration of chlorophyll in the membrane. Taking $c_M = 0.1$ M and an antenna size of $N = 200$ yields $\gamma' = 4.5 \times 10^{-8}\,\text{cm}^3\,\text{s}^{-1}$. This number is within the range of already reported values (Swenberg et al. 1976, Geacintov et al. 1977, Deprez 1986).

Recently we reported on a photoelectric study of trapping and annihilation in PS I in which the photovoltage evoked by 12-ns and 30-ps flashes was also compared (Trissl et al. 1987b). An analogous analysis but with an irreversible reaction scheme of these data yielded a value of $\gamma' = 5.9 \times 10^{-8}\,\text{cm}^3\,\text{s}^{-1}$ (unpublished). The similar values of γ' found for PS I and PS II indicate that this functional parameter is rather independent of the mechanism (irreversible/reversible) and the rate of trapping. It rather indicates the similarity of the antenna systems of the two photosystems of higher plants. However, the faster trapping time in PS I (90 ps) than in PS II (300 ps) causes annihilation effects to be less pronounced in PS I than in PS II.

Trapping kinetics and quantum yield in the low energy limit

The increase of the energy of the picosecond excitation pulse caused a strong decrease of the apparent time constant of trapping (Fig. 2). Two explanations for this dependence can be envisaged. Firstly, annihilation may shorten the lifetime of the excitation in the antenna thereby apparently accelerating the process of trapping. Secondly, if the excitation energy is high enough to close a significant fraction of RCs, the reaction between excitons and open RCs is no longer of first order and the initial trapping rate is proportional to the initial concentration of excitons in the PSU. From the above analysis of the extent of annihilation and the fact that energies up to about 4 hits per trap are used for the data in Fig. 2 and 3, it is expected that both mechanisms contribute. In the general case, bimolecular reactions lead to non-exponential time courses for the exciton decay as well as for the appearance of the charge separated state. Thus our analysis of the data for a monomolecular time constant of the fast rise is an approximation that is strictly valid only in the low energy range of the saturation curve (Fig. 2). The deviations of the data points from the calculated line in the high energy range in Fig. 2 are in part due to this approximation. Another possible explanation was discussed before.

In open PS II units the trapping time in the low energy limit found by photoelectric measurements is $\tau_1 = 300 \pm 30$ ps at low ionic strength and $\tau_1 = 200 \pm 30$ ps (calculated from Table 3) at higher ionic strength. This is within the limit of the values reported for the fast (200–300 ps) fluorescence decay attributed to the trapping time in unfractionated thylakoids with 200–250 Chl/P-680 and in the absence of artificial acceptors (Holzwarth et al. 1985, Schatz and Holzwarth 1987, Keuper and Sauer, 1989). The same trapping time was also found by an indirect measurement of the effect of DNB on fluorescence and photovoltage (Kischkoweit et al. 1988). The faster decay time of the fluorescence kinetics at 8 μJ/cm^2 of 220 ps (Fig. 5a) as compared to the 300 ps trapping time (low energy limit), can be accounted for by annihilations occuring already at this low energy. This was shown by a numerical solution of the set of differential equations [Eqs. (5)–(7)] for $z = 0.08$. The calculations show that the fluorescence decay is generally more sensitive to annihilation than the photovoltage rise (trapping) which is also found in the exciton theory for a lake model with irreversible trapping [Figs. 5 and 6 in Deprez et al. (1989)].

In closed PS II units the trapping time in the low energy limit as determined by the global fit is $\tau_1 = 240 \pm 30$ ps. This surprising acceleration of the trapping time as compared to open RCs is due to the strong increase of k_{-1} that overcompensates the decrease of k_1. In the fluorescence measurements the time constant of the fast phase was longer than expected from the photovoltage rise. This could be due to a non-radiative deactivation path of the radical pair which is not included in our reaction scheme.

A non-radiative deactivation path of a relaxed radical pair state with a time constant of 11 ns was recently proposed by Schlodder and Brettel (1988). However, our finding that more than about 85% of the radical pairs created in closed RCs recombine with a time constant of about 1 ns, excludes that such a reaction contributes significantly in our preparation. A recombination time for the radical pair of 500 ps in a preparation similar to ours was found by spectroscopic measurements (Eckert et al. 1987). This time is predicted by our set of rate constants (Table 3) for higher excitation energies (see Fig. 3).

The parameters obtained from the global fit (Table 3) allow to calculate from Eq. (A.11) the photosynthetic quantum yield of PS II (formation of P-680$^+$ Q_A^-) to be $\Phi_p = 0.62 \pm 0.03$. This yield may be specific for our preparation and the low ionic strength. The increase of the forward rate constants k_1 and k_2 at high ionic strength leads to an increase of the quantum yield to $\Phi_p = 0.8 \pm 0.1$, demonstrating the sensitivity of this photosystem to environmental conditions.

Dielectrically weighted distances

The relative electrogenicity $A_2 = 0.8$–0.9 found in this study for PS II is within the range reported recently (Trissl and Leibl 1989). For purple bacteria A_2 equals 1.5–1.6 (Dobek et al. 1989, Trissl and Leibl 1989, Trissl et al. 1989). Since A_2 corresponds to the dielectrically weighted distance, our result means that the dielectric distance between P-680 and Phe is almost equal to the dielectric distance between Phe and Q_A. Assuming that the geometric positions of the three electron carriers are the same as in purple bacteria (Deisenhofer et al. 1984, Allen et al. 1987), a simple calculation analogous to that made by Trissl et al. (1989) yields for the ratio of the dielectric constants in PS II, $\varepsilon_1/\varepsilon_2 = 0.95 \pm 0.1$. This shows that the dielectric in the RC moiety is more homogenous in PS II than in purple bacteria, for which $\varepsilon_1/\varepsilon_2 = 1.65$ was reported (Trissl et al. 1989).

Conclusions

In the present study the electrogenicity of the back-reaction in the RC of PS II with reduced Q_A was demonstrated for the first time. Furthermore, strong evidence was given for a reversible trapping in closed and open RCs. Thus, the presence of a 'middle' phase (500–650 ps) in fluorescence decay measurements must be ascribed —at least in part —to the reversibility of the trapping process, reflecting the apparent kinetics of charge stabilization. Taking into account a α,β-heterogeneity of PS II with reversible primary photochemistry, the existence of 2 fast and 2 middle phases in fluorescence decay measurements must be expected in intact chloroplasts.

Our data are compatible with the idea that the rates of charge separation as well as of charge stabilization depend on the membrane potential. They also demonstrate sensitive equilibria between the excited states and the primary photochemical states, which are controlled by the redox state of the RC ensemble, probably in a cooperative manner.

The sensitive equilibria might be also affected by the preparation method. This could explain the wide range of reported rate constants. The slow trapping time and the variable reversibility of the charge separation are the molecular basis for a regulation of the turnover rate of PS II under in vivo conditions. In addition to the known regulating mechanism of LHC-phosphorylation, it could well be that PS II is also regulated by PS I via the membrane potential.

Acknowledgements

The authors would like to thank Prof. W. Junge for helpful discussions and continuous support of this work and Mrs. H. Kenneweg for the preparation of PS II membranes and photographs. The financial support by the Deutsche Forschungsgemeinschaft (SFB 171 A1) is acknowledged.

Appendix

At low excitation energy where exciton–exciton annihilation can be neglected (low energy limit) and where all concentrations are much lower than their saturation values, the set of differential equations for the irreversible and the reversible reaction schemes read:

Irreversible scheme	Additional term for reversible scheme	
$dA/dt = -(k_3 + k_1)A$	$+k_{-1}B$	(A.1)
$dB/dt = k_1A - k_2B$	$-k_{-1}B$	(A.2)
$dC/dt = k_2B$		(A.3)

The solutions for the initial conditions $A(0) = A_0 \ll 1$, $B(0)) = C(0) = 0$ are

$$A(t) = A_0[a_1 \exp(-\gamma_1 t) + a_2 \exp(-\gamma_2 t)] \quad (A.4)$$

$$B(t) = A_0[k_1/(\gamma_1 - \gamma_2)][\exp(-\gamma_2 t) - \exp(-\gamma_1 t)] \quad (A.5)$$

$$C(t) = A_0 k_1 k_2/(\gamma_1 - \gamma_2)[1/\gamma_1 \exp(-\gamma_1 t) - 1/\gamma_2 \exp(-\gamma_2 t) + (\gamma_1 - \gamma_2)/(\gamma_1\gamma_2)] \quad (A.6)$$

where the fluorescence amplitudes (a_1, a_2), apparent rate constants (γ_1, γ_2) and the photosynthetic quantum yield (Φ_p) as defined by $\Phi_p = C(t \to \infty)/A_0$ are given by

Irreversible scheme	Reversible scheme	
$a_1^{irr} = 1$	$a_1^{rev} = [\gamma_1 - (k_2 + k_{-1})]/(\gamma_1 - \gamma_2)$	(A.7)
$a_2^{irr} = 0$	$a_2^{rev} = [(k_2 + k_{-1}) - \gamma_2]/(\gamma_1 - \gamma_2)$	(A.8)
$\gamma_1^{irr} = k_1 + k_3$	$\gamma_1^{rev} = (S + \sqrt{S^2 - 4P})/2$	(A.9)
$\gamma_2^{irr} = k_2$	$\gamma_2^{rev} = (S - \sqrt{S^2 - 4P})/2$	(A.10)
$\Phi_p^{irr} = k_1/(k_1 + k_3)$	$\Phi_p^{rev} = (k_1k_2)/(\gamma_1\gamma_2)$	(A.11)

where $S = k_1 + k_{-1} + k_2 + k_3$ and $P = k_{-1}k_3 + k_3k_2 + k_1k_2$ and, in the reversible scheme, γ_1^{rev} and γ_2^{rev} are the solutions of the quadratic equation taken with reversed sign

$$(\gamma^{rev})^2 + \gamma^{rev}(k_1 + k_{-1} + k_2 + k_3) + (k_{-1}k_3 + k_3k_2 + k_1k_2) = 0. \quad (A.12)$$

In the reversible scheme, the following relations are useful for the numerical determination of the molecular rate constants from the measured apparent rate constants

$$\gamma_1^{rev} + \gamma_2^{rev} = k_1 + k_{-1} + k_2 + k_3,$$

$$\gamma_1^{rev}\gamma_2^{rev} = k_{-1}k_3 + k_3k_2 + k_1k_2.$$

The formula for the maximum radical pair concentration is the same for both schemes

$$RP_{max} = A_0k_1/(\gamma_1 - \gamma_2)[(\gamma_1/\gamma_2)^{\gamma_2/(\gamma_2-\gamma_1)} - (\gamma_1/\gamma_2)^{\gamma_1/(\gamma_2-\gamma_1)}]. \quad (A.13)$$

The regeneration process for the photovoltage is the electron transfer connected with a change in the concentrations $B(t)$ and $C(t)$. Under ideal conditions (no distortion by the transmission characteristics of the apparatus) the time dependence of the photovoltage calculates according to

$$V(t) = A_1B(t) + (A_1 + A_2)C(t) \quad (A.14)$$

where A_1 and A_2 are electrogenicity parameters. A_1 correlates with the one between the primary donor, P-680, and pheophytin, Phe, and A_2 with the one between pheophytin and Q_A. For convenience and because the photovoltage is only proportional to concentrations, we set $A_1 = 1$ (i.e. scaling of electrogenicity in units of A_1). Obviously in both schemes $V(t)$ is described by a sum of two exponentials where the amplitudes are functions of the electrogenicity parameters as well as of apparent and molecular rate constants. Since A_2^{irr} is determined in our fits [Eqs. (2a, 2b)], we need the relation

$$(A_2^{rev} + 1)k_2 \equiv (A_2^{irr} + 1)\gamma_2 \quad (A.15)$$

to calculate the electrogenicity factor in the reversible scheme. Equation (A.15) can be derived from Eqs. (A.5), (A.6), and (A.14) and considering that $k_2 = \gamma_2^{irr}$. From this identity it can be seen that whenever k_2 is expected to stay constant (e.g. ± DNB) the fit procedure must conserve the value of the product on the right side of Eq. (A.15), thus saving a fit parameter. If A_2^{irr} and γ_2 are determined under different experimental conditions a change in k_2 can be calculated under the assumption that A_2^{rev} stays constant.

In the linear range of the saturation curve the maximum photovoltage $V_{max} = (A_1 + A_2)C(t \to \infty)$ is proportional to the photosynthetic quantum yield. Once the function $V(t)$ is determined by a fit procedure it is possible to determine $A_1B(t)$ and A_1RP_{max} by setting $A_2 = -A_1 = -1$ [see Eq. (A.14)]. Thus the ratio of RP_{max} under different experimental conditions can be compared.

References

Allen JF, Bennet J, Steinback KE and Arntzen CJ (1981) Chloroplast protein phosphorylation couples plastoquinone redox state to distribution of excitation energy between photosystems. Nature 291: 25–29

Allen JP, Feher G, Yeates TO, Komiya H and Rees DC (1987) Structure of the reaction center from *Rhodobacter sphaeroides* R-26: The cofactors. Proc Natl Acad Sci USA 84: 5730–5734

Berthold DA, Babcock GT and Yoccum CF (1981) A highly resolved, oxygen-evolving photosystem II preparation from spinach thylakoid membranes. FEBS Lett 134: 231–234

Butler WL, Magde D and Berens SJ (1983) Fluorescence lifetimes in the bipartite model of the photosynthetic apparatus with heterogeneity in photosystem II. Proc Natl Acad Sci USA 80: 7510–7514

Carter DP and Staehelin LA (1980) Proteolysis of chloroplast thylakoid membranes. II. Evidence for the involvement of the light-harvesting chlorophyll *a*/*b*-protein complex in thylakoid stacking and for effects of magnesium ions on photosystem II-light-harvesting complex aggregates in the absence of membrane stacking. Arch Biochem Biophys 200: 374–386

Deisenhofer J, Epp O, Miki K, Huber R and Michel H (1984) X-ray structure analysis of a membrane protein complex. Electron density map at 3 Å resolution and a model of the chromophores of the photosynthetic reaction center from *Rhodopseudomonas viridis*. J Mol Biol 180: 385–398

Deprez J (1986) Etude, dans l'échelle de temps subnanoseconde, de la migration et de le capture de l'excitation dans la membrane photosynthétique. Dissertation Université de Paris Sud, Orsay

Deprez J, Paillotin G, Dobek A, Leibl W, Trissl H-W and Breton J (1989) Competition between energy trapping and exciton annihilation in the lake model of the photosynthetic membrane of purple bacteria. Biochim Biophys Acta in press

Deprez J, Trissl H-W and Breton J (1986) Excitation trapping and primary charge stabilization in *Rhodopseudomonas viridis* cells, measured electrically with picosecond resolution. Proc Natl Acad Sci USA 83: 1699–1703

Dobek A, Deprez J, Paillotin G, Leibl W, Trissl H-W and Breton J (1989) Excitation trapping efficiency and kinetics in *Rb. sphaeroides* R26.1 whole cells probed by transmembrane potential measurements in the picosecond time scale. Biochim Biophys Acta in press

Drechsler Z and Neumann J (1987) Membrane charge affecting electron donation to PS II in chloroplasts. Photosynth Res 13: 143–157

Eckert H-J, Renger G, Bernarding J, Faust P, Eichler H-J and Salk J (1987) Examination of fluorescence lifetime and radical-pair decay in photosystem II membrane fragments from spinach. Biochim Biophys Acta 893: 208–218

Eckert H-J, Wiese N, Bernarding J, Eichler H-J and Renger G (1988) Analysis of the electron transfer from $Pheo^-$ to Q_A in PS II membrane fragments from spinach by time resolved 325 nm absorption changes in the picosecond domain. FEBS Lett 240: 153–158

France L, Geacintov NE, Lin S, Wittmershaus BP, Knox RS and Breton J (1988) Fluorescence decay kinetics and characteristics of bimolecular exciton annihilation in chloroplasts. Photochem Photobiol 48: 333–339

Geacintov NE and Breton J (1982) Exciton annihilation and other nonlinear high-intensity excitation effects. In: Biological Events Probed by Ultrafast Laser Spectroscopy, pp 157–191. New York: Academic Press

Geavintov NE and Breton J (1987) Energy transfer and fluorescence mechanisms in photosynthetic membranes. CRC Critical Reviews in Plant Sciences 5: 1–44

Geacintov NE, Breton J, Swenberg CE and Paillotin G (1977) Photochem Photobiol 26: 629–638; Erratum: Photochem Photobiol 29: 651–654

Haehnel W, Nairn JA, Reisberg P and Sauer K (1982) Picosecond fluorescence kinetics and energy transfer in chloroplasts and algae. Biochim Biophys Acta 680: 161–173

Hansson Ö, Duranton J and Mathis P (1988) Yield and lifetime of the primary radical pair in preparations of photosystem II with different antenna size. Biochim Biophys Acta 932: 91–96

Holzwarth AR, Wendler J and Haehnel W (1985) Time-resolved fluorescence spectra of the antenna chlorophylls in *Chlorella vulgaris*. Resolution of photosystem I fluorescence. Biochim Biophys Acta 807: 155–167

Karukstis KK and Monell CR (1989) Reversal of quinone-induced chlorophyll fluorescence quenching. Biochim Biophys Acta 973: 124–130

Karukstis KK and Sauer K (1985) The effects of cation-induced and pH-induced membrane stacking on chlorophyll fluorescence decay kinetics. Biochim Biophys Acta 806: 374–388

Keuper HJK and Sauer K (1989) Effects of photosystem II reaction center closure on nanosecond fluorescence relaxation kinetics. Photosynth Res 20: 85–103

Kischkoweit C, Leibl W and Trissl H-W (1988) Theoretical and experimental study of trapping times and antenna organization in pea chloroplasts by means of the artificial fluorescence quencher *m*-dinitrobenzene. Biochim Biophys Acta 933: 276–287

Kitajima M and Butler WL (1975) Quenching of chlorophyll fluorescence and primary photochemistry in chloroplasts by dibromothymoquinone. Biochim Biophys Acta 376: 105–115

Klimov VV, Allakhverdiev SI and Paschenco VZ (1978) Measurement of activation energy and lifetime of fluorescence of photosystem 2 chlorophyll. Dokl Akad Nauk SSSR 242: 1204–1207

Klimov VV and Krasnovskii AA (1981) Pheophytin as the primary electron acceptor in photosystem 2 reaction centers. Photosynthetica 15: 592–609

Klimov VV and Krasnovskii AA (1982) Participation of pheophytin in the primary processes of electron transfer at the reaction centers of photosystem II. Biophys 27: 186–198

McCauley S and Melis A (1987) Quantitation of photosystem II activity in spinach chloroplasts. Effect of artificial quinone acceptors. Photochem Photobiol 46: 543–550

Meiburg RF, Van Gorkom HJ and Van Dorssen RJ (1983) Excitation trapping and charge separation in photosystem II in the presence of an electrical field. Biochim Biophys Acta 724: 352–358

Moya I, Hodges M, Briantais J-M and Hervo G (1986) Evidence that the variable chlorophyll fluorescence in *Chlamydomonas reinhardtii* is not recombination luminescence. Photosynth Res 10: 319–325

Mullet JE (1983) The amino acid sequence of the polypeptide segment which regulates membrane adhesion (grana stacking) in chloroplasts. J Biol Chem 258: 9941–9948

Mullet J and Arntzen CJ (1980) Simulation of grana stacking in a model membrane system. Mediation by a purified light-harvesting pigment-protein complex from chloroplasts. Biochim Biophys Acta 589: 100–117

Nuijs AM, van Gorkom HJ, Plijter JJ and Duysens LNM (1986) Primary-charge separation and excitation of chlorophyll *a* in photosystem II particles from spinach as studied by picose-

cond absorbance-difference spectroscopy. Biochim Biophys Acta 848: 167–175

Ono T-A and Inoue Y (1985) S-state turnover in the O_2-evolving system of $CaCl_2$-washed photosystem II particles depleted of three peripheral proteins as measured by thermoluminescence. Removal of 33 kDa protein inhibits S_3 to S_4 transition. Biochim Biophys Acta 806: 331–340

Paillotin G, Swenberg CE, Breton J and Geacintov NE (1979) Analysis of picosecond laser-induced fluorescence phenomena in photosynthetic membranes utilizing a master equation approach. Biophys J 25: 513–534

Pearlstein RM (1982) Exciton migration and trapping in photosynthesis. Photochem Photobiol 35: 835–844

Schatz G and Holzwarth AR (1986) Mechanisms of chlorophyll fluorescence revisited: prompt or delayed emission from photosystem II with closed reaction centers? Photosynth Res 10: 309–318

Schatz G and Holzwarth AR (1987) Picosecond time resolved chlorophyll fluorescence spectra from pea chloroplast thylakoids. In: Biggins J (ed) Progress in Photosynth Res, Vol. 1, pp 67–69. Dordrecht: Martinus Nijhoff

Schatz G, Brock H and Holzwarth AR (1987) Picosecond kinetics of fluorescence and absorbance changes in photosystem II particles excited at low photon density. Proc Natl Acad Sci USA 84: 8414–8418

Schatz G, Brock H and Holzwarth AR (1988) Kinetic and energetic model for the primary processes in photosystem II. Biophys J 54: 397–405

Schlodder E and Brettel K (1988) Primary charge separation in closed photosystem II with a lifetime of 11 ns. Flash-absorption spectroscopy with O_2-evolving photosystem II complexes from *Synechococcus*. Biochim Biophys Acta 933: 22–34

Steinback KE, Burke JJ and Arntzen CJ (1979) Evidence for the role of surface-exposed segments of the light-harvesting complex in cation-mediated control of chloroplast structure and function. Arch Biochem Biophys 195: 546–557

Swenberg CE, Geacintov NE and Pope M (1976) Bimolecular quenching of excitons and fluorescence in the photosynthetic unit. Biophys J 16: 1447–1452

Takahashi Y, Hansson Ö, Mathis P and Satoh K (1987) Primary radical pair in the photosystem II reaction center. Biochim Biophys Acta 893: 49–59

Trebst A, Depka B, Kraft B and Johannigmeier U (1988) The Q_B site modulates the conformation of the photosystem II reaction center polypeptides. Photosynth Res 18: 163–177

Trissl H-W, Breton J, Deprez J and Leibl W (1987a) Primary electrogenic reactions of photosystem II as probed by the light-gradient method. Biochim Biophys Acta 893: 305–319

Trissl H-W, Breton J, Deprez J, Dobek A and Leibl W (1989) Trapping kinetics, annihilation, and quantum yield in the photosynthetic purple bacterium *Rps. viridis* as revealed by electric measurement of the primary charge separation. Biochim Biophys Acta in press

Trissl H-W, Gärtner W and Leibl W (1989) Reversed picosecond charge displacement from the photoproduct K of bacteriorhodopsin demonstrated photoelectrically. Phys Chem Lett 158: 515–518

Trissl H-W, Leibl W, Deprez J, Dobek A and Breton J (1987b) Trapping and annihilation in the antenna system of photosystem I. Biochim Biophys Acta 893: 320–332

Trissl H-W and Leibl W (1989) Primary charge separation in photosystem II involves two electrogenic steps. FEBS Lett 244: 85–88

Van Gorkom HJ (1985) Electron transfer in photosystem II. Photosynth Res 6: 97–112

Van Gorkom HJ, Meiburg RF and De Vos LJ (1986) Thermodynamics of the charge recombination in photosystem II. Photosynth Res 9: 55–62

Van Grondelle R (1985) Excitation energy transfer, trapping and annihilation in photosynthetic systems. Biochim Biophys Acta 811: 147–195

Van Grondelle R and Sundström V (1988) Excitation energy transfer in photosynthesis. In: Scheer H and Schneider S (eds) Photosynthetic Light-Harvesting Systems, pp 403–438. Berlin, New York: Walter de Gruyter

Wasielewski MR, Johnson DG, Seibert M and Govindjee (1989) Determination of the primary charge separation rate in isolated photosystem II reaction centers with 500-fs time resolution. Proc Natl Acad Sci USA 86: 524–528

Wendler J and Holzwarth AR (1987) State transitions in the green alga *Scenedesmus obliquus* probed by time-resolved chlorophyll fluorescence spectroscopy and global data analysis. Biophys J 52: 717–728

Zimmermann J-L and Rutherford AW (1986) Photoreductant-induced oxidation of Fe^{2+} in the electron-acceptor complex of photosystem II. Biochim Biophys Acta 851: 416–423

Zinth W, Nuss MC, Polland HJ, Franz MA and Kaiser W (1985) The dynamics of the first steps of the photocycle of bacteriorhodopsin. In: Alix AJP, Bernard L and Manfait M (eds) Spectroscopy of Biological Molecules, pp 325–331. John Wiley & Sons